Generating Particlelike Scattering States in Wave Transport

Stefan Rotter,* Philipp Ambichl, and Florian Libisch
Institute for Theoretical Physics, Vienna University of Technology, A-1040 Vienna, Austria, EU
(Received 18 August 2010; published 25 March 2011)

We introduce a procedure to generate scattering states which display trajectorylike wave function patterns in wave transport through complex scatterers. These deterministic scattering states feature the dual property of being eigenstates to the Wigner-Smith time-delay matrix Q and to the transmission matrix $t^\dagger t$ with classical (noiseless) transmission eigenvalues close to 0 or 1. Our procedure to create such beamlike states is based solely on the scattering matrix and successfully tested numerically for regular, chaotic, and disordered cavities. These results pave the way for the experimental realization of highly collimated wave fronts in transport through complex media with possible applications such as secure and low-power communication.

DOI: 10.1103/PhysRevLett.106.120602 PACS numbers: 05.60.−k, 42.25.−p, 43.20.+g, 73.23.−b

The scattering of waves through complex systems is a central subject in physics occurring on a variety of length and time scales. Coherent electron transport through mesoscopic systems, light transmission through optical devices as well as all matters related to room acoustics are just a few examples of this kind. Recently, enormous experimental progress has been made in the ability to determine the system-specific scattering matrix of such complex systems either explicitly [1] or implicitly by methods like adaptive wave-front shaping [2] and optical phase conjugation [3]. These advances have led to spectacular results for complex scatterers which could be made transparent [2,3] or put to use for focusing an incident wave on a spot size below the diffraction limit [4].

Common to all such applications is the aim to employ the information stored in the scattering matrix to create scattering states with specific properties. A very fundamental property a scattering state can have is to follow the particlelike bouncing pattern of a classical trajectory throughout the entire scattering process [5]. Such ''classical'' scattering states play a key role for the wave-to-particle crossover, for the emergence of geometrical optics out of wave optics, and for the breakdown of universality in coherent transport [6–10]. However interesting these classical states may be, in complex scattering geometries they turn out to be as elusive as the proverbial needle in a haystack.

In this Letter we propose an operational procedure to generate such states explicitly. Our approach is illustrated with the example of a two-dimensional rectangular cavity through which waves can be scattered by two leads attached to the left and right (see Fig. 1). With each lead carrying N open modes the $(2N \times 2N)$-dimensional unitary scattering matrix of this device has the form,

$$S = \begin{pmatrix} r & t' \\ t & r' \end{pmatrix}, \tag{1}$$

where each of the four blocks contains $N \times N$ complex elements for the energy dependent transmission (t) and reflection (r) amplitudes [unprimed (primed) amplitudes designate injection from the left (right) lead]. The total transmission T through this resonant cavity is given as $T = \mathrm{Tr}(t^\dagger t) = \sum_{n=1}^{N} \tau_n$, where the $\tau_n \in [0, 1]$ are the real transmission eigenvalues of the Hermitian matrix $t^\dagger t$. Among the associated eigenstates $|\tau\rangle$ those with eigenvalues close to $\tau = 0$ or $\tau = 1$ are termed ''noiseless states'' as they feature a vanishing contribution to electronic shot noise [6–10]. Since all of the desired classical states with a trajectorylike bouncing pattern must have such deterministic values of transmission they are all part of a highly degenerate noiseless subspace associated with $\tau = 0, 1$.

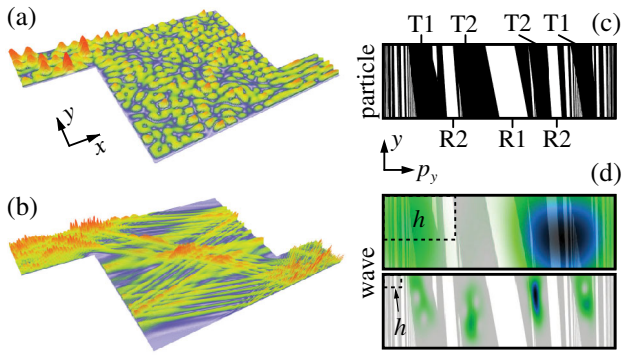

FIG. 1 (color online). Scattering through a rectangular cavity (flux injected through the left lead of width d): (a),(b) Wave function densities of transmission eigenstates $|\tau\rangle$ of $t^\dagger t$ with similar transmission eigenvalues $\tau > 0.99$ but different wave numbers: (a) $k = 5.5\pi/d$, (b) $k = 75.5\pi/d$. (c) Classical surface of section, recorded for trajectories which enter at the left lead mouth with vertical position y and transverse momentum p_y. The largest of the transmission (reflection) bands [black (white)] are labeled by T1, T2 (R1, R2) (bands which are equivalent in an extended zone scheme are given the same label). (d) Husimi distributions of the states shown in (a) (upper panel) and in (b) (lower panel). The size (area) of the Planck cell h is indicated by dashed black frames and the underlying classical phase space is shown in gray.

Consider in Figs. 1(a) and 1(b) two randomly chosen states with $\tau > 0.99$ from this subspace, calculated with the modular recursive Green's function method [11].

The first such state [see Fig. 1(a)] was calculated at a low wave number where only $N = 5$ lead modes are open. To understand the composition of classical trajectories contributing to this state we evaluate the Poincaré surface of section (PSS) at the entrance lead junction [see Fig. 1(c)]. With transmitted (reflected) trajectories being shown in black (white) the PSS features a banded pattern with the individual bands being made up of bundles of trajectories which all have equivalent bouncing patterns [12]. The contributions of different phase space bands to the state $|\tau\rangle$ in Fig. 1(a) are revealed by comparing its quantum phase space distribution (Husimi function) $H(y, p_y) = |\langle\tau|y, p_y\rangle|^2$ with the PSS, where $|y, p_y\rangle$ is a minimum uncertainty state at y, p_y. The corresponding plot in Fig. 1(d) (upper panel) shows that the banded structure of the PSS is not resolved by this state—in line with the fact that the individual areas of the largest phase space bands are all smaller than the Planck constant h, i.e., the lower resolution limit in wave scattering. Rather, this state is composed of many interfering contributions from both transmitting *and* reflecting bands.

The situation is different when, for smaller wave lengths, the size of the Planck cell is well below the size of the largest phase space bands [6–10]. Consider, e.g., the noiseless transmission eigenstate $|\tau\rangle$ with $N = 75$ shown in Fig. 1(b). We find that the Husimi distribution of this state [see Fig. 1(d) (lower panel)] is entirely located on transmission bands, indicating that full transmission is reached here by resolving the classical phase space. Since, however, more than one transmission band contribute (mostly T1 and T2) clear signatures of classical bouncing patterns are still absent in the corresponding scattering wave function [Fig. 1(b)]. This is a result of the indiscriminate mixing of states in the degenerate noiseless subspace. This problem may be circumvented by explicitly constructing scattering states which lie on individual phase space bands [9]. In a real experiment such a protocol, however, meets the problem that the classical phase space structure is typically unknown for a complex scatterer. A viable measurement protocol which is based solely on experimentally accessible quantities like the scattering matrix [1] would thus be highly desirable.

To resolve the contributions of individual phase space bands we present an approach based on the observation that all trajectories in the same band have a characteristic and very similar cavity dwell time. In analogy to eikonal theory we may thus "label" contributions from different bands by their respective dwell times (or path lengths). In wave scattering the closest analogues to classical dwell times are the "proper delay times," i.e., the eigenvalues of the Wigner-Smith time-delay matrix [13],

$$Q = i\hbar \frac{\partial S^\dagger}{\partial E} S = i\hbar \begin{pmatrix} \dot{r}^\dagger r + \dot{t}^\dagger t & \dot{r}^\dagger t' + \dot{t}^\dagger r' \\ \dot{t}'^\dagger r + \dot{r}'^\dagger t & \dot{r}'^\dagger r' + \dot{t}'^\dagger t' \end{pmatrix}, \quad (2)$$

where the dots stand for the energy derivative ∂_E. Using the eigenvalues q_i of Q to lift the unwanted degeneracy in the noiseless subspace is, however, nontrivial since Q has a different dimension ($2N \times 2N$) than the transmission matrix $t^\dagger t$ ($N \times N$). Accordingly, the eigenstates of Q, in general, are scattering states injected from *both* leads, whereas the eigenstates of $t^\dagger t$ are injected from the *left* lead alone. As shown below, this mismatch is conveniently resolved in the noiseless subspace where a basis of common eigenstates to both Q and $t^\dagger t$ can be found.

Because of the Hermiticity of Q its eigenstates $|q_i\rangle$ form an orthogonal and complete set of states, to each of which a real "proper delay time" q_i can be assigned. In the corresponding matrix representation of this eigenproblem, $Q\vec{q}_i^{\,\text{in}} = q_i \vec{q}_i^{\,\text{in}}$, the $2N$-dimensional time-delay eigenvectors $\vec{q}_i^{\,\text{in}} \equiv (\vec{q}_{i,L}^{\,\text{in}}, \vec{q}_{i,R}^{\,\text{in}})$ contain the complex coefficients of the eigenstates $|q_i\rangle$ in the flux-normalized basis of *incoming* modes in the left ($|n\rangle$) and in the right lead ($|n'\rangle$): $(\vec{q}_{i,L}^{\,\text{in}})_n \equiv \langle n|q_i\rangle$ and $(\vec{q}_{i,R}^{\,\text{in}})_{n'} \equiv \langle n'|q_i\rangle$. Correspondingly, the outgoing coefficient vectors $\vec{q}_i^{\,\text{out}} \equiv (\vec{q}_{i,L}^{\,\text{out}}, \vec{q}_{i,R}^{\,\text{out}})$ contain the coefficients in the basis of outgoing modes: $(\vec{q}_{i,L}^{\,\text{out}})_n \equiv \langle \mathcal{T} n|q_i\rangle$ and $(\vec{q}_{i,R}^{\,\text{out}})_{n'} \equiv \langle \mathcal{T} n'|q_i\rangle$, where $\mathcal{T}$ is the time-reversal operator of complex conjugation ($\mathcal{T}^2 = 1$ for spinless scattering). With $\vec{q}_i^{\,\text{out}} = S\vec{q}_i^{\,\text{in}}$ and $S = S^T$ for systems with time-reversal symmetry we define an antiunitarity operator $\Xi = \mathcal{T} S = S^\dagger \mathcal{T}$ which maps the incoming coefficients of a time-delay eigenstate onto the incoming coefficients of the corresponding time-reversed state, $(\vec{q}_i^{\,\text{out}})^* = \Xi \vec{q}_i^{\,\text{in}}$. As this operator Ξ commutes with the time-delay operator, $[\Xi, Q] = 0$ (see [14] A), any *nondegenerate* time-delay eigenstate is time-reversal invariant (up to a global phase $e^{i\alpha}$, $\alpha \in \mathbb{R}$): $\Xi \vec{q}_i^{\,\text{in}} = e^{i\alpha} \vec{q}_i^{\,\text{in}}$. For nondegenerate time-delay eigenstates whose incoming flux from one lead *exits* through both of the leads this time-reversal invariance implies that these states must also have *incoming* flux contributions from both leads. Such $2N$-dimensional time-delay eigenvectors $\vec{q}_i^{\,\text{in}}$ can thus not be reduced to an N-dimensional vector with incoming flux from the left lead alone.

This restriction is lifted in the noiseless subspace, where the *incoming* flux from one lead also *exits* through just one of the leads. Consider a noiseless time-delay eigenstate with fully transmitted incoming flux from the left lead, $t^\dagger t\, \vec{q}_{i,L}^{\,\text{in}} = \vec{q}_{i,L}^{\,\text{in}}$, but no incoming flux from the right lead, $\vec{q}_{i,R}^{\,\text{in}} = \vec{0}$. For this state, $\vec{q}_i^{\,\text{in}} = [\vec{q}_{i,L}^{\,\text{in}}, \vec{0}]$, the commutator $[\Xi, Q] = 0$ implies that the time-reversed state, $\Xi \vec{q}_i^{\,\text{in}} = [\vec{0}, (t\vec{q}_{i,L}^{\,\text{in}})^*]$, is also a time-delay eigenstate with the same eigenvalue q_i as $\vec{q}_i^{\,\text{in}}$. Being a noiseless eigenstate of $t'^\dagger t'$ with incoming flux only from the right lead, $\Xi \vec{q}_i^{\,\text{in}}$ is clearly orthogonal to $\vec{q}_i^{\,\text{in}}$. We thus find that such "noiseless time-delay eigenstates" (NOTEs) come in pairs of two which together form the basis of a doubly degenerate subspace

associated with the time-delay eigenvalue q_i. We emphasize that, in contrast to the common eigenbasis of Ξ and Q in this subspace, $[\vec{q}^{\,\mathrm{in}}_{i,L}, \pm(t\vec{q}^{\,\mathrm{in}}_{i,L})^*]/\sqrt{2}$, NOTEs are not time-reversal invariant. Rather, two NOTEs forming a degenerate pair are the time-reversed of each other like a classical trajectory and its time-reversed partner. Focussing now only on NOTEs injected from the left lead, we can determine their expansion coefficients $\vec{q}^{\,\mathrm{in}}_{i,L}$ with Q from Eq. (2),

$$\begin{pmatrix} Q_{11} & Q_{12} \\ Q_{21} & Q_{22} \end{pmatrix} \begin{pmatrix} \vec{q}^{\,\mathrm{in}}_{i,L} \\ \vec{0} \end{pmatrix} = \begin{pmatrix} Q_{11}\vec{q}^{\,\mathrm{in}}_{i,L} \\ Q_{21}\vec{q}^{\,\mathrm{in}}_{i,L} \end{pmatrix} = q_i \begin{pmatrix} \vec{q}^{\,\mathrm{in}}_{i,L} \\ \vec{0} \end{pmatrix}. \quad (3)$$

For the last equality to hold, the following two conditions need to be fulfilled: (i) $Q_{11}\vec{q}^{\,\mathrm{in}}_{i,L} = q_i\vec{q}^{\,\mathrm{in}}_{i,L}$ and (ii) $Q_{21}\vec{q}^{\,\mathrm{in}}_{i,L} = \vec{0}$. This central result of our Letter implies the following operational procedure to determine the expansion coefficients of NOTEs: In the first step (i) the eigenstates of the Hermitian matrix Q_{11} of dimension $N \times N$ are calculated. Out of this orthogonal and complete set of vectors the subset which, according to (ii), lies in the null-space (kernel) of Q_{21}, constitutes the desired set of common eigenstates of Q and $t^\dagger t$. In practice, condition (ii) can be conveniently verified by a null-space norm $\chi_i = \|Q_{21}\vec{q}^{\,\mathrm{in}}_{i,L}\|$ which determines the degree to which the normalized vector $\vec{q}^{\,\mathrm{in}}_{i,L}$ lies in the null-space of Q_{21}. The quality of a NOTE should be the better the closer this measure $\chi \in [0, \infty]$ is to zero. As the limiting value $\chi \to 0$ is only reached for exact NOTEs with wavelength $\lambda \to 0$, we need to test whether our approach works also for the realistic situation where λ has a finite value.

Consider, as a starting point for such a test, our previous argument that NOTEs can only exist in the noiseless subspace with $\tau = 0, 1$. We emphasize that this requirement, which can similarly not be fulfilled exactly for any finite value of λ, does not explicitly enter conditions (i),(ii) from above. A good indicator for the validity of our approach is thus the degree to which NOTEs with finite values of λ are, indeed, noiseless. For this purpose we calculate the eigenvectors $\vec{q}^{\,\mathrm{in}}_{i,L}$ of Q_{11} [see condition (i)] and verify how the transmission of these states correlates with the corresponding null-space norm χ_i [see condition (ii)]. We find that all eigenstates of Q_{11} which closely fulfill the NOTEs condition (ii) of low χ values are, indeed, either almost fully transmitted, $\tau \approx 1$, or fully reflected, $\tau \approx 0$. This behavior is entirely absent in random matrix theory (RMT) where no phase space bands exist (a comparison of the data for the rectangular cavity with RMT is shown in Fig. 2(a) and in [14] B for other scattering geometries). After these consistency checks we test whether NOTEs with very low null-space norms [$\chi \lesssim 30$, see Fig. 2(a)] display in their wave functions the anticipated pronounced enhancements around individual bundles of classical trajectories. Our results based on the same scattering matrix data as for Fig. 1(b) confirm that states with such low null-space norms χ all feature highly collimated beamlike wave functions [see Figs. 2(b)–2(d) and [14] E). Quite different from arbitrary noiseless states [Figs. 1(a) and 1(b)], NOTEs

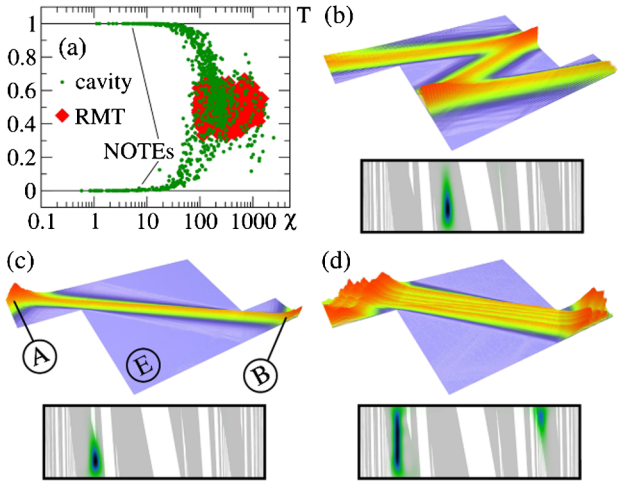

FIG. 2 (color online). (a) Transmission T vs null-space norm χ for eigenstates of the matrix Q_{11} in a rectangular cavity with different lead orientations (green dots). NOTEs with $\chi \to 0$ are noiseless and strongly deviate from RMT (red diamonds, see [14] B for details). (b)–(d) Wave function densities for NOTEs calculated with the same scattering matrix data as used for Fig. 1(b). As demonstrated by the Husimi plots in the bottom panels, each state is located on a single classical phase space band. Null-space projections χ are (b) 4.7, (c) 6.3, (d) 6.9. The insets in (c) illustrate the possibility to use NOTEs for transferring information between a sender (A) and a receiver (B) which bypasses a potential eavesdropper (E).

feature Husimi distributions that do not mix contributions from different phase space bands, thereby corroborating the successful operation of our procedure. Without exception we find that in cases where NOTEs seem to feature contributions from more than one band [as in Fig. 2(d)] all these bands belong to a single connected band in an extended zone scheme [like T1/T2/R2 in Fig. 1(c)] [12].

Our numerical results indicate furthermore that the proper delay times of NOTEs do not only lift the degeneracy of noiseless states located on *different* bands, but that also the small dwell-time differences between trajectories of the *same* band do get increasingly well resolved in the limit $\lambda \to 0$. Correspondingly, we find that the proper delay times q_i of NOTEs on the *same* band are characteristically different from each other (rather than degenerate). NOTEs thus fill individual phase space bands in a well-controlled fashion. Consider, e.g., the band T1: starting from the state in Fig. 2(c) the proper delay times and the transverse quantization of states on this band increase [see, e.g., Fig. 2(d)] until, when the band is filled, the null-space norm of states increases substantially (see [14] E), indicating a substantial overlap with phase space outside of the band. Such an increase in χ values is often found to be accompanied by signatures of diffractive scattering at the sharp lead mouths (see [14] E).

Since the operational procedure presented here does not rely on any specific assumptions concerning the type of scattering in a given system, we also applied it to more complex scattering geometries. Consider first the

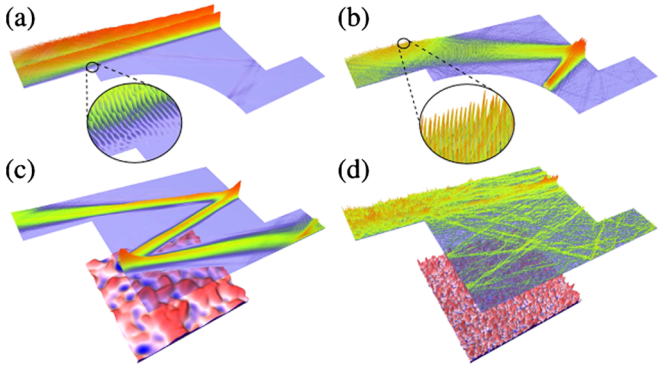

FIG. 3 (color online). NOTEs at $k = 75.5\pi/d$ in cavities (a), (b) with a Sinai-type boundary shape and (c),(d) with a bulk disorder of amplitude $V_0/E = 0.1$ (see illustrations). The correlation of the disorder is long-range for (c) with correlation length $kr_c = 30\pi$ and short-range for (d) where $kr_c = 5\pi$. Null-space norms χ are (a) 1.7, (b) 24.8, (c) 4.9, (d) 65.7.

Sinai-type billiard structure in Figs. 3(a) and 3(b) which features chaotic classical dynamics due to scattering at the circular part of the hard wall potential. We find that NOTEs which do not have any overlap with the curved part of the boundary [see Fig. 3(a)] have wave functions and proper delay times as in the rectangular cavity. For comparison, we also show in Fig. 3(b) a state which bounces off the circular boundary. As reflected in its increased null-space norm ($\chi = 24.8$) the high instability of this state's bouncing pattern makes it much harder to resolve the (small) area of its phase space band. Consider next rectangular cavities containing a static disorder potential with correlation length r_c and an average amplitude V_0. By studying such disordered cavities we find that our approach is restricted to the limit of weak and long-range disorder, $V_0/E \ll 1$ and $kr_c \gg 1$ (in agreement with the validity criterion for the WKB/eikonal approximation [15] and previous work [10]). Correspondingly, for the same fixed disorder amplitude ($V_0/E = 0.1$) the z-shaped scattering state from Fig. 2(b) survives in the presence of long-range disorder [see Fig. 3(c)], whereas no such state exists for short-range correlations [see Fig. 3(d) for the state with the closest time-delay value and [14] B, E for more details).

We have performed additional tests (see [14] C) to verify that all NOTEs which we find within the above limits are associated with individual classical trajectory bundles. This feature allows for a WKB/eikonal-type ansatz for the transmission matrix of NOTEs, $t \approx \vec{q}_{i,R}^{\,\text{out}} e^{iS_b(E)/\hbar} \vec{q}_{i,L}^{\,\text{in}\dagger}$, in which the only part with a significant energy dependence is the action phase, $S_b(E) = \int_b \vec{k} d\vec{l}$, accumulated along bundle b. We show in [14] D that this ansatz fulfills the defining conditions for NOTEs (i),(ii) from above.

We believe that our results open up many interesting possibilities for the experiment, where the cavities considered here could, e.g., be an acoustic resonator (like a room) or an electromagnetic scatterer (like closely spaced buildings). In both these cases the collimated wave functions associated with NOTEs could be used to transfer information between a sender (A) and a receiver (B) such that the power to generate the signal is minimized and the transmitted signal is kept out of reach of an eavesdropper (E) [see illustration in Fig. 2(c)]. In this sense NOTEs offer clear advantages over arbitrary noiseless scattering states that do not display such beamlike wave functions in general [see, e.g., Figs. 1(a) and 1(b)]. NOTEs may also have interesting connections to phenomena in closed or decaying systems [16–18].

In summary, we present an operational procedure for constructing scattering states which follow classical bouncing patterns in coherent transport through cavities or complex scattering landscapes. In analogy to WKB/eikonal theory we find that such ray-optical or beamlike scattering states are determined by the condition of a fixed scattering time delay. Our procedure is generally applicable to different types of wave scattering (acoustic, electromagnetic, quantum, etc.) and relies solely on the knowledge of the scattering matrix.

We wish to thank F. Aigner, J. Burgdörfer, A. Cresti, and A. Foerster for helpful discussions. Support by the WWTF and computational resources by the Vienna Scientific Cluster (VSC) are gratefully acknowledged.

*Corresponding author: stefan.rotter@tuwien.ac.at

[1] S. M. Popoff *et al.*, Phys. Rev. Lett. **104**, 100601 (2010).
[2] I. M. Vellekoop and A. P. Mosk, Phys. Rev. Lett. **101**, 120601 (2008).
[3] Z. Yaqoob *et al.*, Nat. Photon. **2**, 110 (2008).
[4] I. M. Vellekoop, A. Lagendijk, and A. P. Mosk, Nat. Photon. **4**, 320 (2010).
[5] P. Ehrenfest, Z. Phys. **45**, 455 (1927).
[6] P. G. Silvestrov, M. C. Goorden, and C. W. J. Beenakker, Phys. Rev. B **67**, 241301 (2003).
[7] J. Tworzydlo *et al.*, Phys. Rev. B **68**, 115313 (2003).
[8] P. Jacquod and E. V. Sukhorukov, Phys. Rev. Lett. **92**, 116801 (2004).
[9] P. Jacquod and R. S. Whitney, Phys. Rev. B **73**, 195115 (2006).
[10] S. Rotter, F. Aigner, and J. Burgdörfer, Phys. Rev. B **75**, 125312 (2007).
[11] S. Rotter *et al.*, Phys. Rev. B **62**, 1950 (2000); **68**, 165302 (2003).
[12] L. Wirtz, J.-Z. Tang, and J. Burgdörfer, Phys. Rev. B **56**, 7589 (1997).
[13] L. Reichl, *The Transition to Chaos* (Springer, New York, 2004), 2nd ed..
[14] See supplemental material at http://link.aps.org/supplemental/10.1103/PhysRevLett.106.120602 where details on the derivations as well as a statistical analysis and additional wave functions of NOTEs are provided.
[15] R. J. Glauber, *Lectures in Theoretical Physics* (Interscience, New York, 1959), Vol. 1, p. 315.
[16] E. G. Vergini *et al.*, Europhys. Lett. **89**, 40013 (2010).
[17] M. Kopp and H. Schomerus, Phys. Rev. E **81**, 026208 (2010).
[18] H. E. Türeci *et al.*, Opt. Express **10**, 752 (2002).